Supplementary Information for

Fluorescence Correlation Spectroscopy of Phosphatidylinositol-specific Phospholipase C Monitors the Interplay of Substrate and Activator Lipid Binding[†]

Mingming Pu[‡], *Mary F. Roberts*[‡] *and Anne Gershenson*[§,*].

[‡]Department of Chemistry, Boston College, Boston, MA 02467. [§]Department of Chemistry, Brandeis University, Waltham, MA 02454

Low X_{PC} and Sigmoidal Binding Curves

At low X_{PC} (<0.5), the curves for PI-PLC binding to SUVs are often sigmoidal, suggesting that a minimum cluster of PC headgroups is required for binding (1). This is illustrated in Figure S1 for *Y88A binding to SUVs with X_{PC} = 0.3. The experimental points are shown for low phospholipid concentrations to emphasize the sigmoidal nature of the curve. The solid line is the fit to Equation 2 with a fitted value of n =1.8±0.1, while the dashed line is the hyperbolic (n=1) fit. Using a cooperative versus a hyperbolic fit has minor effects on the extracted K_d, which is 0.52±0.02 mM with the cooperative equation and 0.65±0.13 mM with the hyperbolic fit.

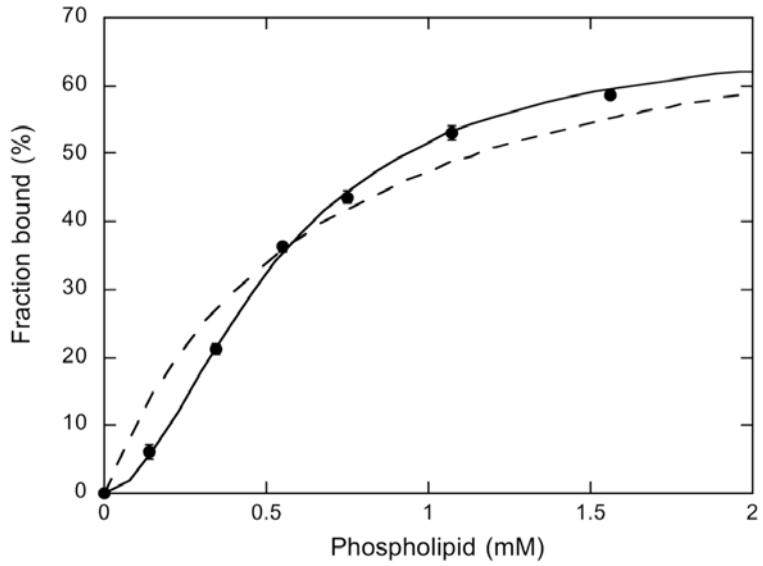

*Figure S1. *Y88A binding to PG/PC SUVs with X_{PC} =0.3.*

FCS and SUV size distributions

There are currently no good, widely available methods for producing SUVs with a truly narrow size distribution. The SUVs used for the PI-PLC experiments were prepared by sonication and show a size distribution that is skewed towards smaller vesicles (1). The SUV size

distribution for these studies depends on lipid composition. Due to the bigger PC headgroup, vesicles containing only PC are larger on average than those containing only PG and thus have smaller diffusion coefficients (Figure S2). The vesicle radius, R, is related to the diffusion coefficient, D_{SUV}, by the Stokes-Einstein equation $D_{SUV}=k_BT/(6\pi\eta R)$ where k_B is the Boltzmann constant, T is temperature in Kelvin and η is the viscosity of water (0.955 mPa s at 22 C). Pure PC SUVs exhibit an average radius, <R>, of 16 nm corresponding to $<D_{SUV}>$ =14 $\mu m^2/s$ while pure PG vesicles have <R> of 10 nm and $<D_{SUV}>$=23 $\mu m^2/s$ (Figure S1). SUVs composed of a PC:PG mixtures fall between these two extremes.

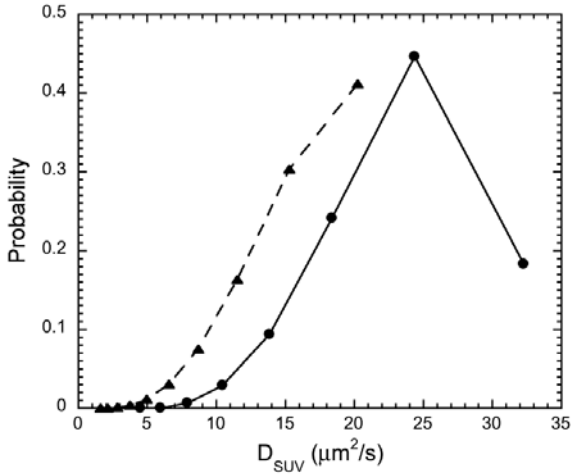

Figure S2. D_{SUV} probability distributions for pure PG (●) and pure PC (▲) SUVs determined from dynamic light scattering data (1). Larger diffusion coefficients correspond to smaller vesicles.

How do these distributions affect the correlation curves for proteins binding to SUVs? Taking the SUV distributions into account, the correlation, G(τ), is expressed as:

$$G(\tau)=\frac{1}{\langle N\rangle}\left(\begin{array}{l}(1-f)\left[\left(1+\frac{\tau}{\tau_{free}}\right)\sqrt{1+\frac{\tau}{S^2\tau_{free}}}\right]^{-1}\\ +f\sum_j P(\tau_{bound,j})\left[\left(1+\frac{\tau}{\tau_{bound,j}}\right)\sqrt{1+\frac{\tau}{S^2\tau_{bound,j}}}\right]^{-1}\end{array}\right) \qquad (S1)$$

where <*N*> is the time averaged number of PI-PLC molecules in the effective volume, τ_{free} and τ_{bound} are the diffusion times for free and vesicle-bound PI-PLC respectively, and *S* is the ratio of the axial (z) to the radial (x-y) dimension for the effective volume. The diffusion time for each

species is given by $\tau_{species}=\omega_o^2/4D_{species}$ where ω_o is the radius of the observation volume in the x-y plane. The probability that the protein binds to a particular size vesicle and that this vesicle is detected in an FCS experiment is given by $P(\tau_{bound,j})$. This probability is a convolution of at least three probabilities: (i) the relative population of SUVs with a particular size, (ii) the probability that the protein will bind to a particular size vesicle, and (iii) the probability of detecting different sized vesicles with different fluorescence intensities (brightnesses). Because these probabilities are not easily measured, they could be determined from fits to the correlation curves. Fitting the probabilities would, however, lead to grossly underconstrained fits; therefore, we and others (1-3) have instead fit SUV binding data to a 2 species model with a single value for τ_{bound} (Equation 1 in the main text).

How does this 2 species approximation affect the values of K_d and the maximum fraction bound, f_{max}? To determine this, we calculated $G(\tau)$ using the D_{SUV} distribution from either the pure PG or pure PC light scattering data (Figure S2 and Equation S1). The characteristics of the protein and the effective volume were based on the experimentally determined values with D_{free}=56 $\mu m^2/s$, ω_o=0.24 μm and S=7. To mimic a titration experiment, $G(\tau)$ was calculated for f values ranging from 0 (no protein bound to SUVs) to 1 (100% binding). Each model value of f is associated with a total phospholipid concentration, [PL], using:

$$f = f_{max}[PL]/ (K_d + [PL]) \qquad (S2)$$

for f_{max}=1 and K_d=10 μM. Changing the value of K_d does not alter the conclusions described below (data not shown).

2 Species Fits to the Model Correlation Curves. In analogy to the experimental analysis, the correlations calculated using the SUV size distributions were analyzed using a 2 species fit (equation 1, main text) with D_{free}, ω_o and S fixed to the values used in the model calculations, and D_{bound} either fixed or globally fit for each set of modeled titration curves (Figure S3). Fits were performed with the ISS Vista program used to fit the experimental data. As expected, the deviation of the residuals from zero increases as the percent binding increases and the SUV size distribution makes a greater contribution to the correlation. Fits using fixed values of D_{bound} that are larger than the D_{bound} obtained from global fits tend to overestimate $G(\tau)$ at times shorter than the diffusion time and underestimate $G(\tau)$ at times that are close to the diffusion time (top

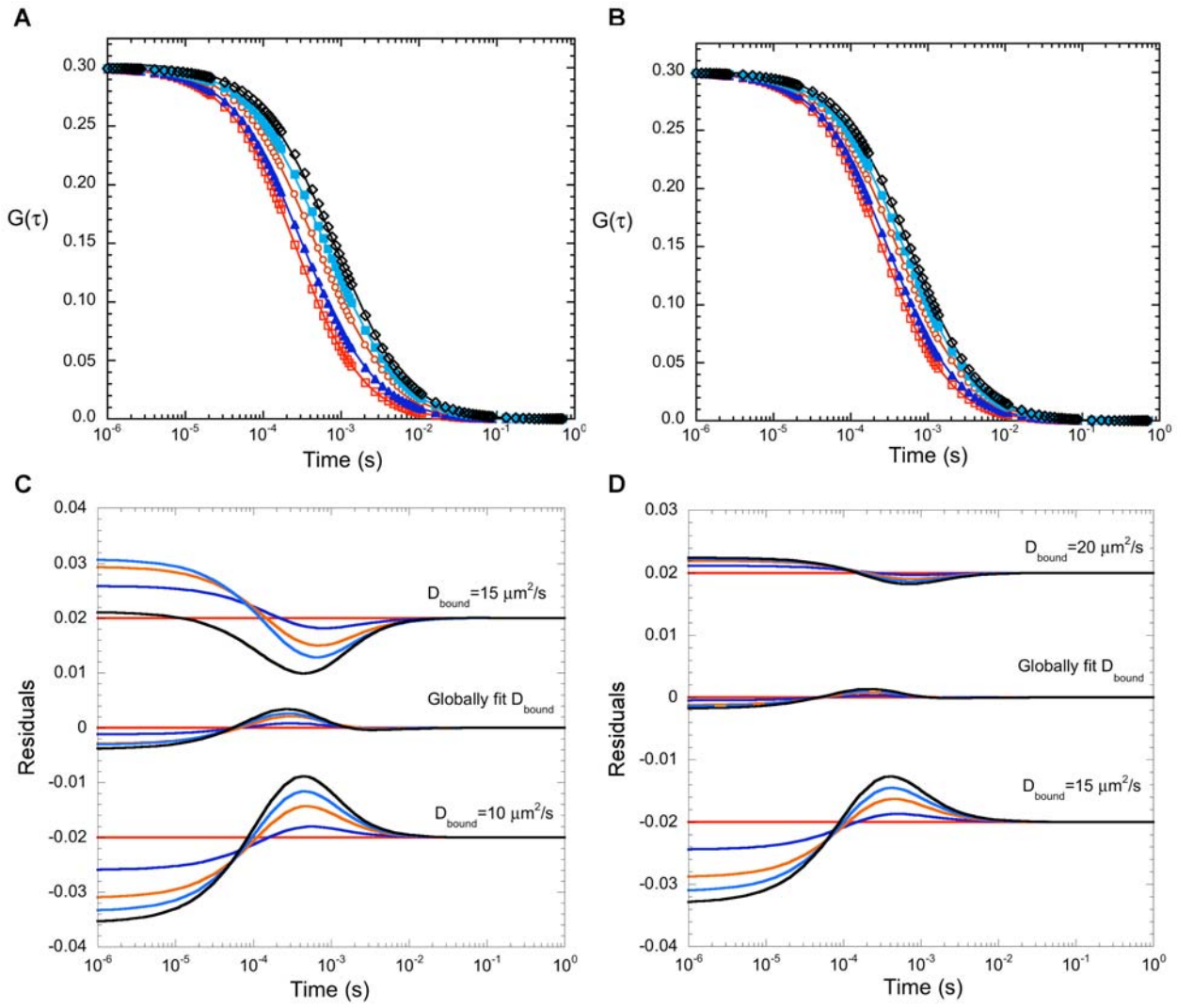

Figure S3. Model correlation curves (symbols) for 0 (red), 20 (blue), 50 (orange), 70 (light blue) and 90 (black) percent binding. The model data were calculated using the pure PC SUV size distribution (A) or the pure PG SUV size distribution (B). The lines are 2 species fits to the data when globally fitting D_{bound}. The results for D_{bound} are 11.9±0.1 and 18.5±0.1 $\mu m^2/s$ for the pure PC and pure PG distributions respectively. (C & D). Residuals for the 2 species fits to the pure PC model data (C) and pure PG model data (D). The middle residual plots are for globally fitting D_{bound}, the fits shown in (A) and (B). The top and bottom residuals, offset for clarity, are from fits using fixed values of D_{bound} with the top residuals for D_{bound} = 15 and 20 $\mu m^2/s$ and the bottom residuals for D_{bound} = 10 and 15 $\mu m^2/s$ for the PC and PG distributions, respectively.

residuals Figures S3C and S3D). In contrast, globally fitting D_{bound}, or fixing D_{bound} to small values yield the opposite trend, underestimating $G(\tau)$ at times shorter than the diffusion time and overestimating $G(\tau)$ at times close to the diffusion time. Unfortunately, no such trends are observed in fits to the experimental data. This discrepancy may be due to PI-PLC's preference for smaller vesicles (1, 4) which would alter the underlying distribution as well as to experimental noise that contributes to the experimental residuals.

Both the experimental and model data show an interesting trend when the correlation curves are globally fit to determine D_{bound}. The global fitting can be performed using the full set of titration data or in pieces for the beginning and end of the titration curve, e.g. the data for samples containing 0 to 50 μM phospholipid binding can be globally fit separately from the data for >50 μM phospholipid. If the second method is used, the fitted value of D_{bound} increases with the phospholipid concentration. For example, for the pure PC model correlation curves, D_{bound} goes from 11.8 $\mu m^2/s$ for data with <50% binding (low phospholipid concentrations) to 12.0 for data with >50% binding, while for the pure PG model data D_{bound} goes from 18.4 to 18.6 $\mu m^2/s$. While these changes are quite small, they are consistently observed for global 2 species fits to the model and the experimental data, and may be an indication that a binding partner has a significant distribution of sizes.

Determining f_{max} and K_d. In order to determine how the 2 species fits affect the values determined for f_{max} and K_d, the fraction bound determined from the 2 species fits, f_{2sp}, were used to construct titration curves which were then fit to equation S2 (Figure S4). The 2 species fits to the model data show that f_{max} is quite sensitive to the fitting method and generally asymptotes at values that are less than 100% (Figure S4, Table S1). Surprisingly, f_{max} is linearly dependent on the ratio $D_{bound}/\langle D \rangle$ (Figure S4C) where $\langle D \rangle$ is the average value of the SUV diffusion coefficient determined from the probability distributions shown in Figure S2. As this ratio increases, the value obtained for f_{max} from the hyperbolic fits increases. The 2 species fits using values of D_{bound} 25% higher than $\langle D \rangle$ were the only fits that yielded f_{max} values on the order of 100%. However, such high values of D_{bound} lead to poor fits to the correlation curves as shown by the large residuals in Figure S3C. Thus, good fits to the experimental correlation curves will likely result in values of f_{max} that are significantly less that 100% due to the 2 species approximations.

Globally fitting D_{bound} for these model SUV size distributions results in f_{max} of about 80%. For the experimental data, globally fitting D_{bound} results in values of f_{max} between 50 and 60%. The values determined for f_{max} depend on how the correlation curves are fit and the underlying distribution of detected SUVs. In experiments, the SUV distribution is affected not only by the distribution of SUV sizes but also by preferential binding of PI-PLC and differences in detection efficiency. In addition, the experimental data also contains noise whereas the model data are noiseless. Thus, it is difficult to predict what experimental values of f_{max} represent 100% binding. Nonetheless, the fact that the experimental values of f_{max} are significantly less than 100% agrees with the model predictions.

In contrast, values obtained for K_d for both model and experimental data are quite robust (Table S1). For the pure PC distribution, fits using a fixed value of D_{bound} that is 25% higher than <D> results in a low value for K_d and an f_{max} that is greater than 100% (Table S1). At the opposite extreme, using fixed, low values for D_{bound} results in low values of f_{max} without significantly affecting K_d. This analysis shows that while the value f_{max} depends on $D_{bound}/\langle D \rangle$, for good fits to the correlation curves K_d has no such dependence and is usually within 5% of the actual value for the model data.

These modeling results suggest that for vesicles with a large distribution of sizes, K_d values from 2 species fits are likely to be reliable but values of f_{max} are not. These results also explain why fits to the experimental data, either using fixed values of D_{SUV} or globally fitting D_{SUV} rarely show 100% binding. Based on this modeling, we suggest that that the accuracy of K_d for data involving a wide distribution of vesicle sizes be evaluated by fitting the correlation curves to 2 species fits using fixed values of D_{SUV} as well as by globally fitting D_{SUV}. The fixed values of D_{SUV} should bracket the average value expected based on the distribution of vesicle sizes. The K_ds obtained using these different fitting strategies should be similar and reliable while values obtained for f_{max} are likely to be significantly less than 100% even in the presence of 100% binding. If the K_ds deviate significantly between fitting strategies, a more complicated fitting equation with more adjustable parameters may be necessary. These results should be applicable not only to SUV binding studies, but to any FCS binding studies where one of the species has a distribution of shapes and/or sizes which significantly affects the diffusion times.

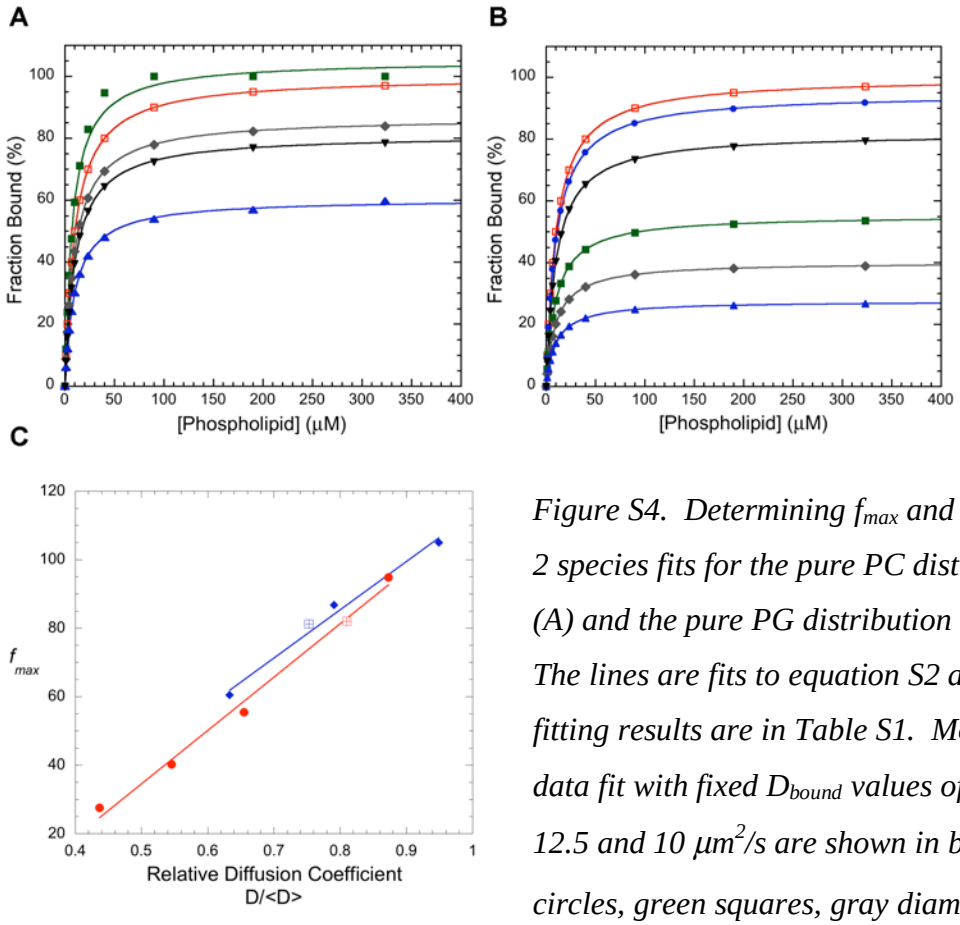

Figure S4. Determining f_{max} and K_d from 2 species fits for the pure PC distribution (A) and the pure PG distribution (B). The lines are fits to equation S2 and the fitting results are in Table S1. Model data fit with fixed D_{bound} values of 20, 15, 12.5 and 10 $\mu m^2/s$ are shown in blue circles, green squares, gray diamonds and blue triangles respectively. Model data for which D_{bound} was globally fit is shown in black triangles, and the calculated points and fit for f_{max}=1 and K_d=10 μM, the model values, are shown in red. (C) The dependence of f_{max} on the value of D/<D> for the pure PC distribution (blue diamonds) and the pure PG distribution (red circles). The lines are linear fits to the data. The squares are the results from globally fitting D_{bound} and were not included in the linear fits.

Table S1. The results of fitting f_{2sp} versus [PL] curves (Figure S4) to equation S2.

	Pure PC Distribution **<R>=16.2 nm** **$<D_{SUV}>$ = 15.8 μm²/s**		***Pure PG Distribution*** **<R>=10.8 nm** **$<D_{SUV}>$ = 22.9 μm²/s**	
	K_d (μM)	**f_{max} (%)**	**K_d (μM)**	**f_{max} (%)**
Calculated	10.0	100	10.0	100
Fix D_{bound}=20 μm²/s	NA[1]	NA[1]	10.1	94.8
Fix D_{bound}=15 μm²/s	7.54	105	9.97	55.4
Fix D_{bound}=12.5 μm²/s	9.97	86.8	9.94	40.2
Fix D_{bound}=10 μm²/s	10.1	60.5	9.90	27.6
Globally fit D_{bound}	10.4	81.2	10.3	82.0

[1] Not applicable, D_{bound}=20 μm²/s is too large for the pure PC distribution

[2] The globally fitted values for D_{bound} are 11.9±0.1 μm²/s and 18.5±0.1 μm²/s for pure PC and pure PG distributions respectively.

References:

1. Pu, M., Fang, X., Redfield, A. G., Gershenson, A., and Roberts, M. F. (2009) Correlation of vesicle binding and phospholipid dynamics with phospholipase C activity: Insights into phosphatidylcholine activation and surface dilution inhibition, *J. Biol. Chem.*, *284,* 16099-16107.
2. Takakuwa, Y., Pack, C.-G., An, X.-L., Manno, S., Ito, E., and Kinjo, M. (1999) Fluorescence correlation spectroscopy analysis of the hydrophobic interactions of protein 4.1 with phosphatidyl serine liposomes, *Biophys. Chem. 82,* 149-155.
3. Lu, L., Ding, J. L., Ho, B., and Wohland, T. (2005) Investigation of a novel artificial antimicrobial peptide by fluorescence correlation spectroscopy: An amphipathic cationic pattern is sufficient for selective binding to bacterial type membranes and antimicrobial activity, *Biochim. Biophys. Acta 1716,* 29-39.
4. Wehbi, H., Feng, J., Kolbeck, J., Ananthanarayanan, B., Cho, W., and Roberts, M.F. (2003) Investigating the interfacial binding of bacterial phosphatidylinositol-specific phospholipase C, *Biochemistry 42,* 9374-82.